Facilitating the EPR Effect and Improving Tumor Penetration and Nanoparticle Delivery with Ultrafine Iron Oxide Nanoparticle as Observed via Its Dual-Contrast Effect

Jing Huang[1,2], Liya Wang[1,2], Hui Wu[1,2], Lily Yang[3], and Hui Mao[1,2]

[1]*Laboratory of Functional-Molecular Imaging and Nanomedicine, Emory University School of Medicine, Atlanta, GA, United States,* [2]*Radiology and Imaging Sciences, Emory University School of Medicine, Atlanta, Georgia, United States,* [3]*Surgery, Emory University, Atlanta, GA, United States*

Purpose

Nanomaterials are widely used for developing tumor targeted molecular imaging probes and drug delivery systems. Engineered nanoparticles, typically in the range of 10-100 nm (core size), are delivered to the tumor based on the enhanced permeability and retention (EPR) effect. However, this is often affected by their size, shape, stiffness, surface charge and surface properties [1]. Optimizing and controlling the physical/chemical properties of the nanoparticles can improve the delivery efficiency and tumor accumulation. Here we report the findings of sub-5 nm ultrafine iron oxide nanoparticles (uIONP) with a core diameter of 3.5 nm and dual T_1-T_2 contrast facilitating the EPR effect, resulting higher tumor tissue penetration and accumulation, resulting improved passive tumor targeting and MRI contrast enhancing when delivered to the tumor.

Materials and Methods

Oligosaccharides coated iron oxide nanoparticles with a core size of 3.5 nm (uIONP) were prepared according to the previous developed method [2]. To study the pH responsive properties, the hydrodynamic size and surface charge changes of uIONP at different pH conditions were observed by dynamic light scattering (DLS) and zeta potential measurements. To investigate the changes in MRI relaxivities caused by pH modulation, IONPs solutions with different concentrations and different pH conditions were examined by a 3T MRI scanner using T_1- and T_2-weighted fast spin echo sequences, inversion recovery (IR) turbo spin echo sequence and multi-echo T_2-weighted spin echo sequence. R_1 and R_2 relaxivities were calculated by fitting signal changes in multi-IR T_1 and multi-TE T_2 images using simple exponential equations. Protein and liposome encapsulated uIONP micelles were tested for their MRI contrast effect in clustered forms. The dual T_1-T_2 contrast and their switch caused by aggregation of uIONP were further validated by in vitro experiment. Macrophage (RAW264.7) cells were labelled with SIOs with sizes of 3.5 nm or 20 nm, respectively, following TEM and MRI analysis, compared with the cells lysed after labelling. To study the passive tumor targeting and accumulation properties, IONPs with different sizes (i.e. 3.5, 10, 20 nm) were intravenously administered into mice bearing tumors of 4T1 breast cancer. Fat suppressed T_1- and T_2-weighted spin echo images were obtained to investigate the contrast changes in major organs and tumors at the different time points. Ex vivo biodistribution studies were performed to determine the tumor accumulation, including iron concentration measurement by the colorimetric method and Prussian blue staining for sliced organs/tumors. To further investigate the penetration of uIONP into the tumor, uIONPs were labelled with a red fluorescent dye TRITC, whereas IONP with 20 nm size (IO20) were labelled with green FITC. Mixture of uIONP-TRITC and IO20-FITC was intravenously injected into mice bearing 4T1 breast cancer. The tumor tissue penetration of nanoparticles was observed under a confocal microscope after collecting and slicing the tumor.

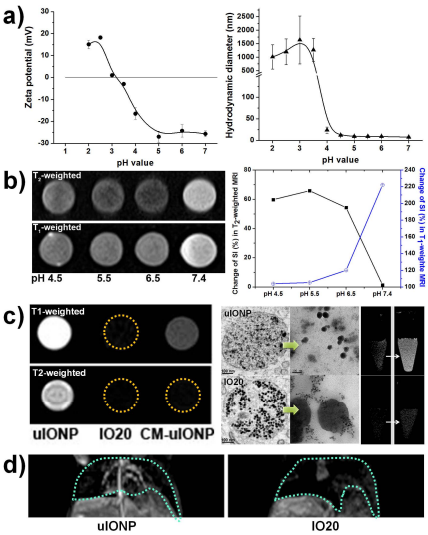

Fig. 1. (a) pH-responsive properties of uIONP. (b) Signal intensity changes of T_1- and T_2-weighted MR images of uIONP at different pHs. (c) T_1-T_2 switch when uIONPs compartmentalize in different environment is observed when uIONPs encapsulated in micelle (T_2) or cells and released (T_1). (d) Dual contrast in T_1-weighted liver MR images.

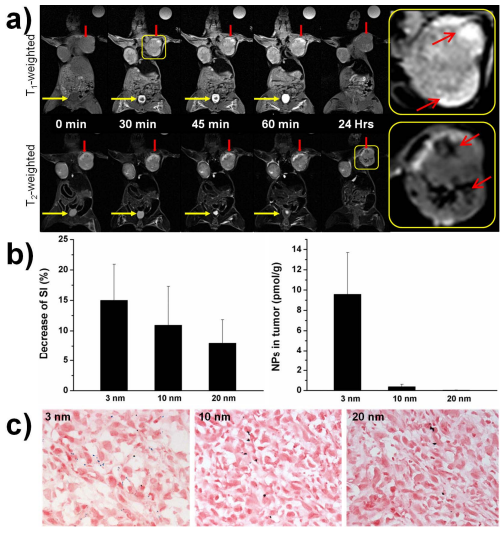

Fig. 2. (a) T_1- and T_2-weighted MRI of a mouse injected with uIONPs. (b) The percentage of signal intensity (SI) decrease in T_2-weighted MRI for the mice injected with IO in different sizes, and the corresponding iron contents (right panel) measured by the colorimetric method show the higher accumulation of uIONPs. (c) The representative Prussian blue staining of the tumor section, in which iron was represent as blue dots.

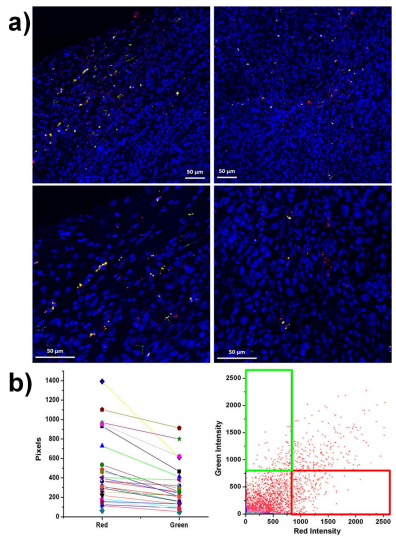

Fig. 3. (a) Representative fluorescent images of tumor section from mice injected with uIONP-TRITC (red) and IO20-FITC (green), showing the greater accumulation of uIONP both at the tumor edge and deeper site. (b) A representative plot shows the distribution and co-localization of uIONP-TRITC and IO20-FITC.

Results and Discussions

DLS and zeta potential measurements showed that the prepared uIONP has an isoelectric point at pH 3.1 (**Fig. 1**). The hydrodynamic size increased when pH decreased to below 5.5 because uIONPs became clustering due to decreased surface charge impulsion. At pH 5.5, uIONP exhibited an enhanced T_2 effect in T_2-weighted MR images after forming clusters, comparing to that at pH 7.4. The clustered uIONPs in the protein micelle showed a lower r_1 and a higher r_2 as predicted, compared with single dispersed uIONPs. TEM images of macrophages labelled with IONPs revealed that IONPs were engulfed and internalized in the lysosome of the cells. In contrast to the darken T_1-weighted MR images of the labelled cells where uIONPs clustered intracellularly, "bright" T_1 contrast was observed when the labelled cells were lysed and uIONPs were released and re-dispersed in the media. MRI of mice receiving i.v. injection of uIONPs further demonstrated the capacity of dual T_1-T_2 contrast effect in vivo. For example, blood vessels were enhanced in T_1-weighted imaging after injection of uIONP; however, hepatic tissues became darkened because of T_2 effect from the accumulation and clustering of uIONP in the liver. Tumor bearing mice received uIONPs showed T_1 contrast enhancing with higher SI in the tumor peripheral first (<60 mins), however, uIONPs assembled in the tumor interstitial space, evidenced by T_2 contrast and SI decrease in the tumor at the later time points (e.g. 24 h, **Fig. 2**). Although clustering uIONPs led to a lower r_2 value than larger IO20s, it showed greatest decrease of SI in the tumor site at 24 h after systemic administration, as a result of the largest accumulation amount compared to IONPs with a larger size (10, 20 nm). Confocal microscope analysis of tumor tissue from the mice receiving co-injection of 3.5 nm and 20 nm IONPs labelled with different fluorescent dyes (red vs. green) revealed that the tumors received uIONPs had more than 1.6 fold increase of the iron content compared to larger sized nanoparticles (**Fig. 3**).

Conclusions

Ultrafine iron oxide nanoparticles were studied for their pH-responsive and assembly properties that led to novel MRI contrast properties in vivo and in vitro. More importantly, uIONPs exhibited greater tumor accumulation in 4T1 mouse model, demonstrated by both MRI and confocal images, mainly due to maximizing the EPR effect with easy extravasations at a sub-5 nm size and then clustering in the tumor interstitial space to prevent re-entering the ciruclation, thus enhancing the passive targeting delivery. Furthermore, the T_1-T_2 contrast switch depending on the compartmentalization of uIONPs may provide a mechanism for MRI monitoring the nanovehicle delivery process in vivo.

References: 1. Sun T, et al, *Angew. Chem. Int. Ed.* 2014, 53, 12320-12364; 2. Huang, J. et al. *J. Mater. Chem. B*, 2014, 2, 5344–5351.

Grant Support: This work is supported in parts by the grants R01CA154846-02 and U01CA151810-03 from National Institutes of Health.